Journal of Medicinal Chemistry

Article

Design, Synthesis, and Biological Evaluation of Dual Binding Site Acetylcholinesterase Inhibitors: New Disease-Modifying Agents for Alzheimer's Disease

Pilar Muoz-Ruiz, Laura Rubio, Esther Garca-Palomero, Isabel Dorronsoro, Mara del Monte-Milln, Rita Valenzuela, Paola Usn, Celia de Austria, Manuela Bartolini, Vincenza Andrisano, Axel Bidon-Chanal, Modesto Orozco, F. Javier Luque, Miguel Medina, and Ana Martnez

J. Med. Chem., **2005**, 48 (23), 7223-7233• DOI: 10.1021/jm0503289 • Publication Date (Web): 13 October 2005

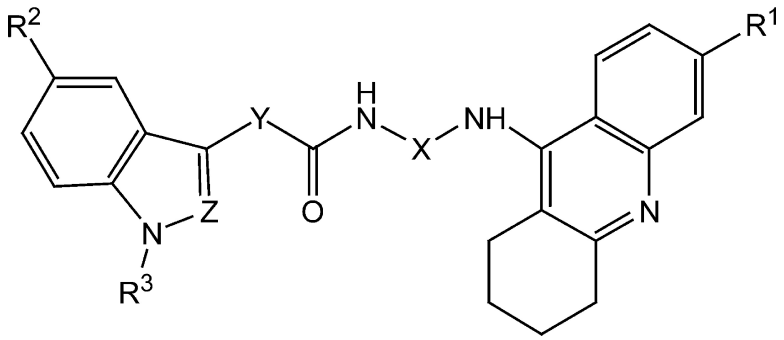

More About This Article

Additional resources and features associated with this article are available within the HTML version:

- Supporting Information
- Links to the 8 articles that cite this article, as of the time of this article download
- Access to high resolution figures
- Links to articles and content related to this article
- Copyright permission to reproduce figures and/or text from this article

View the Full Text HTML

Journal of Medicinal Chemistry is published by the American Chemical Society. 1155 Sixteenth Street N.W., Washington, DC 20036

Design, Synthesis, and Biological Evaluation of Dual Binding Site Acetylcholinesterase Inhibitors: New Disease-Modifying Agents for Alzheimer's Disease

Pilar Muñoz-Ruiz,[§] Laura Rubio,[§] Esther García-Palomero,[§] Isabel Dorronsoro,[§] María del Monte-Millán,[§] Rita Valenzuela,[§] Paola Usán,[§] Celia de Austria,[§] Manuela Bartolini,[‡] Vincenza Andrisano,[‡] Axel Bidon-Chanal,[#] Modesto Orozco,[†] F. Javier Luque,[#] Miguel Medina,[§] and Ana Martínez*[,§]

Neuropharma, S.A., Avda. de La Industria 52, 28760 Tres Cantos, Madrid, Spain, Department of Pharmaceutical Sciences, University of Bologna, Via Belmeloro 6, 40126 Bologna, Italy, Departamento de Fisicoquímica, Facultad de Farmacia, Universidad de Barcelona, Avda. Diagonal 643, 08028 Barcelona, Spain, and Departamento de Bioquímica y Biología Molecular, Facultad de Química, Universidad de Barcelona, Martí i Franqués 1, 08028 Barcelona, Spain

Received April 11, 2005

New dual binding site acetylcholinesterase (AChE) inhibitors have been designed and synthesized as new potent drugs that may simultaneously alleviate cognitive deficits and behave as disease-modifying agents by inhibiting the β-amyloid (Aβ) peptide aggregation through binding to both catalytic and peripheral sites of the enzyme. Particularly, compounds **5** and **6** emerged as the most potent heterodimers reported so far, displaying IC_{50} values for AChE inhibition of 20 and 60 pM, respectively. More importantly, these dual AChE inhibitors inhibit the AChE-induced Aβ peptide aggregation with IC_{50} values 1 order of magnitude lower than that of propidium, thus being the most potent derivatives with this activity reported up to date. We therefore conclude that these compounds are very promising disease-modifying agents for the treatment of Alzheimer's disease (AD).

Introduction

Alzheimer's disease (AD), the most common form of neurodegenerative senil dementia, is associated with selective loss of cholinergic neurons and reduced levels of acetylcholine neurotransmitter, and it is characterized by loss of memory and progressive impairment in cognitive functions.[1] Post-mortem brain studies, specially in neurocortex and hypocampus regions, have revealed the presence of several distinct neuropathological hallmarks, including extracellular β-amyloid (Aβ) containing plaques, intracellular neurofibrillary tangles containing abnormally hyperphosphorylated τ protein, and degeneration of cholinergic neurons of the basal forebrain.[2]

In the past 2 decades, enormous research effort has been spent to understand the molecular pathogenesis of AD, thus providing a robust framework to develop effective pharmacological treatments.[3] However, the only therapeutic approach currently approved exploits the enhancement of the central cholinergic function,[4] which increasees the acetylcholine levels in the brain. Thus, over the past decade various cholinergic drugs, primarily inhibitors of the enzyme acetylcholinesterase (AChE) such as tacrine,[5] donepezil,[6] rivastigmine,[7] and more recently galantamine[8] (Figure 1), have been launched on the market for the symptomatic treatment of AD.

The therapeutic potential of AChE inhibitors has been strengthened by evidence showing that, besides their role on the cognitive function, they might contribute to slow the neurodegeneration in AD patients. In fact, it is known that AChE exerts secondary noncholinergic functions,[9] related to its peripheral anionic site,[10,11] in cell adhesion[12,13] and differentiation,[14] and recent findings also support its role in mediating the processing and deposition of Aβ peptide;[15−18] AChE is one of the proteins that colocalizes with Aβ peptide deposits in the brain of AD patients[15] and promotes Aβ fibrillogenesis by forming stable AChE−Aβ complexes.[16] Additionally, it has also been postulated that AChE binds through its peripheral site to the Aβ nonamyloidogenic form and acts as a pathological chaperone inducing a conformational transition to the amyloidogenic form.[17,18] On the basis of this evidence, dual binding site AChE inhibitors appear to be promising for the design of new antidementia drugs, since they might simultaneously alleviate the cognitive deficit in AD patients and act as disease-modifying agents delaying the amyloid plaque formation.[19,20] Following this rationale, new AChE inhibitors

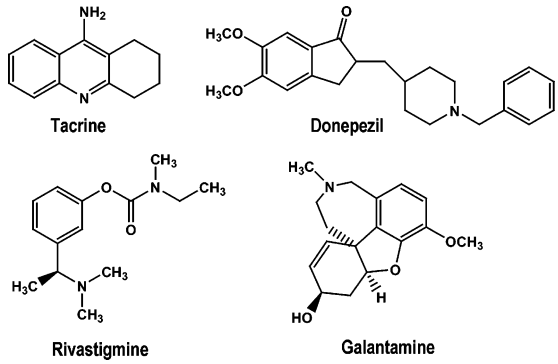

Figure 1. AChE inhibitors clinically used for the treatment of AD.

* To whom correspondence should be addressed. Phone: +34 91 8061130. Fax: +34 91 8034660. E-mail: amartinez@neuropharma.es.
[§] Neuropharma, S.A.
[‡] University of Bologna.
[#] Departamento de Fisicoquímica, Universidad de Barcelona.
[†] Departamento de Bioquímica y Biología Molecular, Universidad de Barcelona.

10.1021/jm0503289 CCC: $30.25
Published on Web 10/13/2005

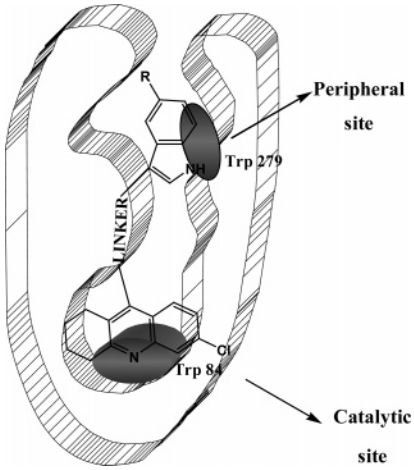

Figure 2. Indole−tacrine heterodimers binding simultaneously to the catalytic and peripheral sites of the AChE.

have been designed to interact simultaneously with both catalytic and peripheral sites.[21−24]

Continuing with our search for new dual-binding site AChE inhibitors,[25−27] we report here the design, synthesis, and pharmacological evaluation of a new series of potent compounds containing in their structures a 1,2,3,4-tetrahydroacridine fused ring (tacrine) as the catalytic anionic site binding unit, and an indole ring as the peripheral site binding unit, connected to each other by a linker of suitable length and nature (Figure 2).[28] The tacrine unit was, in previous studies, incorporated in a series of bis-tacrines, designed by Pang et al,[19] that showed high potency and selectivity in AChE inhibition, being up to 248-fold more selective and 149-fold more potent than tacrine. Since then, tacrine has been incorporated into several families of AChE dual inhibitors.[29−31] Because the insertion of chlorine into position 6 of tacrine enhances the affinity toward AChE,[32] we have also combined the 6-chlorotacrine unit with the indole ring unit in most of the synthesized heterodimers. The indole ring moiety was chosen on the basis of its pharmacological, structural, and electronic properties. In this view, the indole ring linked to the tacrine moiety by a tether of appropriate length could reach the entrance of the catalytic gorge and interact with the Trp279 by $\pi-\pi$ stacking.[33,34] To our knowledge, the indole unit has been incorporated only once into a dual binding site AChE inhibitor, in the case of tryptamine in combination with tacrine, which resulted in 3-fold less potency than tacrine.[35] Regarding the linker, we first synthesized indole−tacrine inhibitors containing a propionamide moiety linked to position 3 of the indole ring and to an alkylaminotacrine of different methylene tether length. The influence of the linker on the pharmacological activity was explored by different chemical modifications: (i) conformational restriction at the propionamide chain, (ii) inclusion of an additional *N*-Me function in the central part of the methylene chain linked to tacrine, (iii) variation of the relative position of the carbonyl group and the heterocyclic units, and (iv) replacement of the amide group by a carbamate residue, which is present in other AChE inhibitors such as rivastigmine. Finally, derivatives containing other heterocycles such as 5-cyanoindole, 5-bromoindole, *N*-methylindole, and indazole derivatives were also synthesized.

The AChE and BChE inhibitory activity of each compound was evaluated, and their selectivity ratio (AChE/BChE) was also calculated. A molecular modeling study was performed to determine the binding mode of these dual inhibitors to the AChE. Furthermore, for those compounds showing very promising disease-modifying profiles for the treatment of AD, their Aβ_{1-40} peptide aggregation inhibitory activity and their AChE-induced Aβ_{1-40} peptide aggregation inhibitory activity were studied to confirm their dual action. Finally, cytotoxicity studies were performed in human neuroblastoma cells.

Chemistry

The synthetic methodology employed for the preparation of the new dual binding site heterodimers was varied depending on the carbonylic bond type (amide or carbamate) in the linker, which is inserted in the last step of the synthetic pathway, as depicted in Schemes 1 or 2, respectively. Preparation of the new dual heterodimers containing an amide bond, compounds **3**−**23** (Table 1), was carried out by coupling the required 9-alkylaminotetrahydroacridines **1a**−**i** to the corresponding indole carboxylic acid derivatives **2a**−**i**, employing 1,1-carbonyldiimidazol (CDI) as coupling agent (Scheme 1).[36] The 9-alkylaminotetrahydroacridines **1a**−**i** of different tether lengths were readily obtained following the reported methodology.[30] All the indole carboxylic acid derivatives **2** employed for the preparation of the new dual heterodimers **3**−**23** were commercially available except for 5-cyanoindole-3-propionic acid (**2b**), which was synthesized according to a reported methodology.[37] Thus, activation of the indole carboxylic acid derivatives **2** with CDI in THF for about 4 h followed by treatment with the corresponding 9-alkylaminotetrahydroacridines **1a**−**i** generated the desired dual binding site inhibitors **3**−**23** in yields ranging from 8% to 97%. In general, the yield of the reaction decreases dramatically as the number of methylene units of the 9-alkylaminotetrahydroacridines **1** varies from 8 (**7**, 53%) to 10 (**9**, 19%). The presence of an electron-withdrawing group at position 5 of the indole ring, compounds **2b** and **2f**, seemed to decrease the activation of the carboxylic group, since compounds **12** (22%) and **19** (54%) were obtained in much lower yields than their unsubstituted analogues **5** (77%**)** and **18** (84%). Coupling the indole-3-propenoic acid (**2c**) to the 9-alkylaminotetrahydroacridines **1c** resulted in low formation of the heterodimer **13** (8%), probably because of the conjugation of the double bond with the carboxylic acid group that might reduce the nucleophilicity of the hydroxyl group. Heterodimers **14**−**17**, containing an amide group directly attached to the indole fused-ring, were also obtained in moderate yield as observed when comparing **16** (51%) with **18** (80%) and **6** (79%), where the carbonylic group is separated by one or two methylene groups from the indole ring, respectively. This effect was even more remarkable at synthesizing the heterodimers **22** (8%) and **23** (13%), which also contain an amide directly connected to the *N*-Me indole and indazole rings, respectively.

Regarding the synthesis of the new heterodimers containing a carbamate functionality within the linker (Scheme 2), we designed a synthetic approach in which

Scheme 1[a]

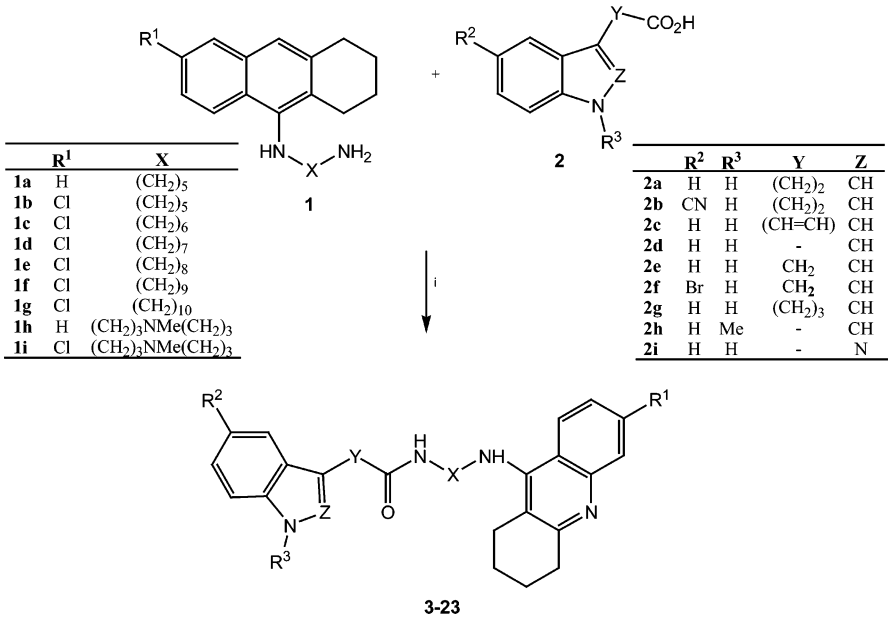

	R^1	X
1a	H	$(CH_2)_5$
1b	Cl	$(CH_2)_5$
1c	Cl	$(CH_2)_6$
1d	Cl	$(CH_2)_7$
1e	Cl	$(CH_2)_8$
1f	Cl	$(CH_2)_9$
1g	Cl	$(CH_2)_{10}$
1h	H	$(CH_2)_3NMe(CH_2)_3$
1i	Cl	$(CH_2)_3NMe(CH_2)_3$

	R^2	R^3	Y	Z
2a	H	H	$(CH_2)_2$	CH
2b	CN	H	$(CH_2)_2$	CH
2c	H	H	(CH=CH)	CH
2d	H	H	-	CH
2e	H	H	CH_2	CH
2f	Br	H	CH_2	CH
2g	H	H	$(CH_2)_3$	CH
2h	H	Me	-	CH
2i	H	H	-	N

[a] Reagents: (i) 1,1′-carbonyldiimidazole, THF.

Scheme 2[a]

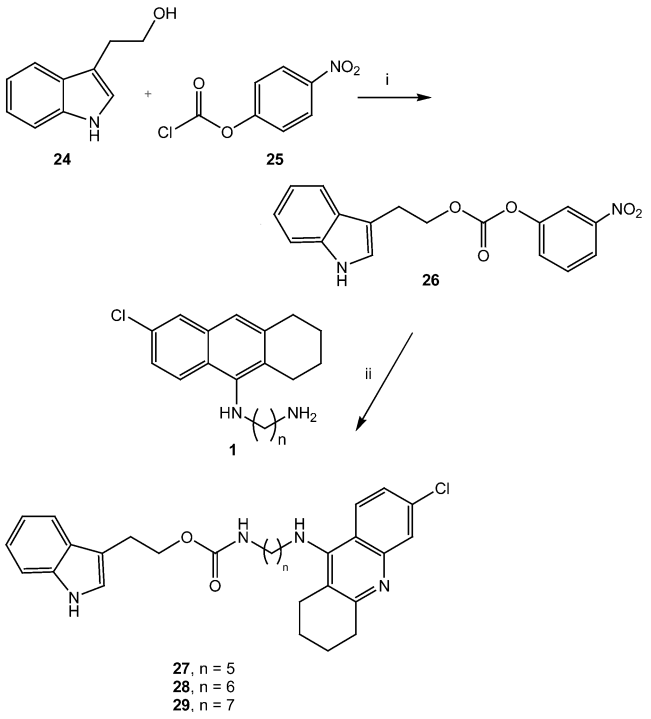

[a] Reagents: (i) *N*-methylmorpholine; (ii) DMAP, DMF.

preparation of the highly reactive intermediate phenyloxycarbonyl derivative **26** was required before coupling to the corresponding 9-alkylaminotetrahydroacridines **1**.[38] Thus, the carbonate intermediate **26** was prepared in 32% yield by treatment of 2-(1*H*-indol-3-yl)ethanol (**24**) with *p*-nitrophenyl chloroformate (**25**) in *N*-methylmorpholine, followed by chromatographic purification. Finally, treatment of the carbonate derivative **26** with the corresponding 9-alkylaminotetrahydroacridines **1b**−**d** in the presence of DMAP resulted in the formation of the carbamate derivatives **27**−**29** that were then purified by chromatography.

The chemical structures of all new compounds synthesized herein were fully characterized by analytical and spectroscopic data reported in the Experimental Section. Bidimensional spectroscopic experiments $^1H-^1H$ COSY and $^1H-^{13}C$ HMQC, and $^1H-^{13}C$ HMBC were carried out for unequivocal assignment of the chemical shifts observed in the ^1H and ^{13}C NMR spectra. The molecular weights of all compounds synthesized were confirmed by low-resolution mass spectrometry analysis ESI^+ (electrospray), and their degree of purity was also determined by elemental and HPLC analyses.

Results and Discussion

AChE Inhibitory Activity. To determine the therapeutic potential of this new series of tacrine−indole heterodimers (compounds **3**−**23** and **27**−**29**) for the treatment of AD, their AChE inhibitory potency was assayed on AChE from bovine erythrocytes according to Ellman et al.,[39] using tacrine as a reference compound. With only the exception of compound **14**, the tacrine−indole heterodimers were all clearly more active as bovine AChE inhibitors than the parent compound tacrine (see Table 1). In particular, compounds **5** and **6** were >8000- and >2500-fold, respectively, more potent than tacrine. As previously reported in the literature,[40] insertion of a chlorine atom at position 6 of tacrine leads to a large enhancement in the binding affinity, 6-chlorotacrine heterodimers **4** and **11** being 17- and 49-fold more potent than their unsubstituted analogues **3** and **10**, respectively.

With the aim of optimizing the interaction of the heterodimers with both catalytic and peripheral binding sites of AChE, both the length of the tether and the position of the amide group within the linker were varied. Thus, among the heterodimers bearing two methylene groups between the indole ring and the amide functionality, those in which the tether length from the amide to the tacrine unit contains 6 or 7 methylenes (compounds **5** and **6**) displayed the best AChE inhibitory activity (see Table 1). This potency

Table 1. Inhibition of AChE and BChE Activities and Selectivity Ratios Determined for the Indole−Tacrine Heterodimers

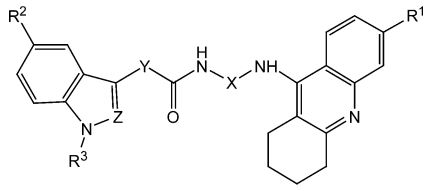

compd	R^1	R^2	R^3	X	Y	Z	IC_{50}(AChE)[a] (nM)	IC_{50}(BChE)[a] (nM)	selectivity AChE/ BChE
tacrine							167 (119−233)	24 (12−45)	6.9
3	H	H	H	$(CH_2)_5$	$(CH_2)_2$	CH	70 (54−95)	1 (0.8−1.5)	70
4	Cl	H	H	$(CH_2)_5$	$(CH_2)_2$	CH	4 (3−6)	16 (8−31)	0.25
5	Cl	H	H	$(CH_2)_6$	$(CH_2)_2$	CH	0.02 (0.01−0.03)	2.9 (1.1−7.5)	0.007
6	Cl	H	H	$(CH_2)_7$	$(CH_2)_2$	CH	0.06 (0.04−0.10)	0.1 (0.06−0.13)	0.6
7	Cl	H	H	$(CH_2)_8$	$(CH_2)_2$	CH	0.5 (0.3−1.0)	5.7 (3.7−8.7)	0.09
8	Cl	H	H	$(CH_2)_9$	$(CH_2)_2$	CH	4.4 (2.7−6.8)	9.6 (3−25)	0.4
9	Cl	H	H	$(CH_2)_{10}$	$(CH_2)_2$	CH	21.9 (16−29)	54 (30−97)	0.4
10	H	H	H	$(CH_2)_3NMe(CH_2)_3$	$(CH_2)_2$	CH	147 (100−202)	0.03 (0.01−0.06)	4900
11	Cl	H	H	$(CH_2)_3NMe(CH_2)_3$	$(CH_2)_2$	CH	2.9 (2.2−3.8)	21.4 (12−37)	0.13
12	Cl	CN	H	$(CH_2)_6$	$(CH_2)_2$	CH	0.7 (0.3−1.4)	11.7 (5−23)	0.06
13	Cl	H	H	$(CH_2)_6$	(CH=CH)	CH	18 (12−26)	77 (50−120)	0.2
14	Cl	H	H	$(CH_2)_5$		CH	180 (95−350)	9.5 (7−12)	18.9
15	Cl	H	H	$(CH_2)_6$		CH	33 (20−53)	1.7 (0.9−3)	19
16	Cl	H	H	$(CH_2)_7$		CH	36 (18−70)	19 (12−28)	1.9
17	Cl	H	H	$(CH_2)_8$		CH	46 (23−83)	22.4 (13−37)	2.1
18	Cl	H	H	$(CH_2)_7$	CH_2	CH	0.2 (0.11−0.29)	11.7 (6.4−21)	0.02
19	Cl	Br	H	$(CH_2)_7$	CH_2	CH	0.6 (0.4−1.0)	1.7 (1.0−2.7)	0.3
20	Cl	H	H	$(CH_2)_5$	$(CH_2)_3$	CH	0.3 (0.2−0.5)	3.2 (1.7−6.1)	0.09
21	Cl	H	H	$(CH_2)_6$	$(CH_2)_3$	CH	0.5 (0.2−0.9)	5.6 (3.5−8.8)	0.09
22	Cl	H	Me	$(CH_2)_7$		CH	10.9 (6.6−17)	206 (145−292)	0.05
23	Cl	H	H	$(CH_2)_7$		N	95 (53−170)	79 (63−97)	1.2
27	Cl	H	H	$(CH_2)_5$	$(CH_2)_2O$	CH	1.5 (1.0−2.3)	136 (87−212)	0.1
28	Cl	H	H	$(CH_2)_6$	$(CH_2)_2O$	CH	0.7 (0.4−1.0)	60 (41−86)	0.2
29	Cl	H	H	$(CH_2)_7$	$(CH_2)_2O$	CH	3.0 (2.0−4.4)	59 (43−81)	0.05

[a] 95% confidence intervals are given in parentheses.

decreases as the number of methylene units is lengthened from 8 to 10 (compounds **7**−**9**) or decreased to 5 (compound **4**). Replacement of the central methylene group of heterodimer **6** by a methylamine group decreases the AChE inhibitory activity of compound **11**, which is nearly 50-fold less potent. Moreover, conformational restriction of heterodimer **5** by introduction of unsaturation at the linker also substantially reduces the AChE binding affinity, as noted by the fact that compound **13** is about 900-fold less potent than **5**. All these findings suggest that along the gorge the tether must satisfy very specific structural requirements to allow the interaction of both tacrine and indole units at both catalytic and peripheral binding sites. Finally, the 5-cyanoindole heterodimer **12** was about 35-fold less potent than the unsubstituted analogue **5**.

Regarding the family of heterodimers where the carbonyl group is directly attached to the indole ring, the AChE inhibitory activity was similar for heterodimers bearing six, seven, and eight methylene units within the linker (compounds **15**−**17**). However, shortening the length of the tether to five methylenes (**14**) leads to a notable decrease in the inhibitory potency. Furthermore, compounds **16** and **17**, which possess the same number of methylene units as **4** and **5** but differ in the position of the amide group within the linker, are clearly less potent, being particularly worse for compound **17**, which is around 2300-fold less potent than **5**. This result strongly suggests that the location of the amide group within the linker is critical. Further support of this conclusion comes from the comparison of the potencies determined for heterodimers **18** and **5**. Though the total length of the linker is identical in the two compounds, compound **18** is around 10-fold less potent than **5**, which must be attributed to the fact that in the former compound the amide group is separated by only one methylene from the indole ring. Likewise, when the amido group is separated by three methylenes from the indole ring (compounds **20** and **21**), the inhibitory activity drops 10-fold with respect to **5** and **6**, though the total length of tether is maintained. Thus, the precise location of the amido group plays a decisive role in modulating the inhibitory potency of the heterodimer.

Replacement of the methylene adjacent to the carbonyl group in heterodimers **20** and **21** by an oxygen (compounds **27** and **28**) did not produce an important variation in the inhibitory activity. Similarly, replacement of the indole ring in **16** by an indazole ring (**23**) or methylation of the indole nitrogen atom (**22**) has modest effects on the inhibitory potency.

On the basis of the preceding results, heterodimers **5**, **6**, and **18**−**20**, which were the most potent inhibitors in bovine erythrocyte AChE, were also assayed in human brain AChE. Within the uncertainty of the experimental measurements, the results confirm the trends mentioned above (see Table 2). Thus, compounds **5** and **6** have similar inhibitory activities, which are close to the values determined for bovine AChE. Moreover, compounds **18**−**20** exhibit similar potencies, being 2- to 10-fold less active than compounds **5** and **6**. These results, therefore, confirm that these tacrine−indole heterodimers possess very potent activities with IC_{50} values at subnanomolar levels.

Table 2. Inhibition of Human AChE by Selected Indole−Tacrine Heterodimers

compd	IC_{50}(AChE)[a] (pM)	K_i(AChE)[a] (pM)	selectivity AChE/BChE
5	70 (0.4−1.0)	14 (3−20)	0.02
6	20 (10−30)	9 (2−17)	0.22
18	120 (80−180)	15 (4−20)	0.01
19	230 (140−370)	20 (8−30)	0.14
20	130 (80−200)	1.7 (−0.7−4)	0.04

[a] 95% confidence intervals are given in parentheses.

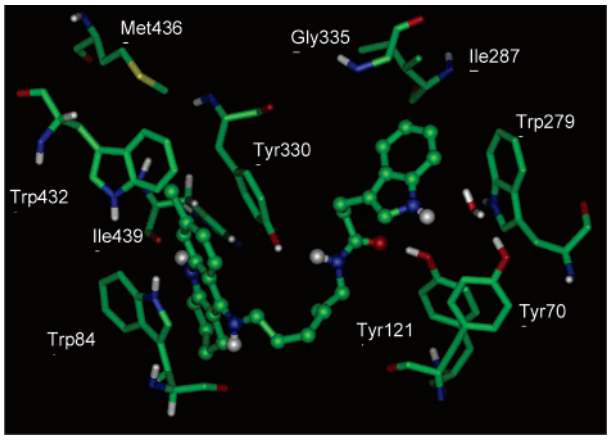

Figure 3. Representation of the heterodimer **5** docked into the binding site of AChE highlighting the protein residues that form the main interactions with the different structural units of the inhibitor.

Molecular Modeling. To gain insight into the molecular determinants that modulate the inhibitory activity, a molecular modeling study was performed to explore the binding of heterodimer **5** to the enzyme (see Experimental Section for details).

The position of heterodimer **5** with respect to the key residues in the binding site is shown in Figure 3. The tacrine moiety is firmly bound to the catalytic site of AChE, it being stacked against the aromatic rings of Trp84 and Tyr330 (average distances between rings: 3.52 (Trp84) and 3.56 (Tyr330) Å). The aromatic nitrogen of tacrine is hydrogen-bonded to the main-chain carbonyl oxygen of His440 (average N···O distance: 2.84 Å). In addition, a hydrogen-bond interaction is also formed along the simulation between the tacrine amino NH group and the main-chain carbonyl oxygen of Trp84 (average N···O distance: 3.27 Å). Finally, the chlorine atom occupies a small hydrophobic pocket formed by Trp432, Met436, and Ile439. This feature, which has been identified in both modeling studies[41] and the X-ray crystallographic structure[42] of the AChE−huprine Y complex, justifies the higher potencies of heterodimers having the 6-chlorotacrine unit compared to the unsubstituted compounds.

With regard to the linker, which is aligned along the gorge, the most relevant feature comes from the interactions formed by the amido group. Thus, the NH group is hydrogen-bonded to the hydroxyl oxygen of Try330 (average N···O distance: 3.01 Å), which in turn remains firmly stacked onto the tacrine unit. Indeed, the carbonyl oxygen is hydrogen-bonded to the hydroxyl oxygen of Tyr121 (average O···O distance: 2.75 Å). Overall, the presence of the amido group in the tether permits us to define a network of interactions that couple several residues of the enzyme gorge and different structural units of the inhibitor, thus explaining the notable dependence of the inhibitory potency on the position of the amido group within the tether (see above and Table 1).

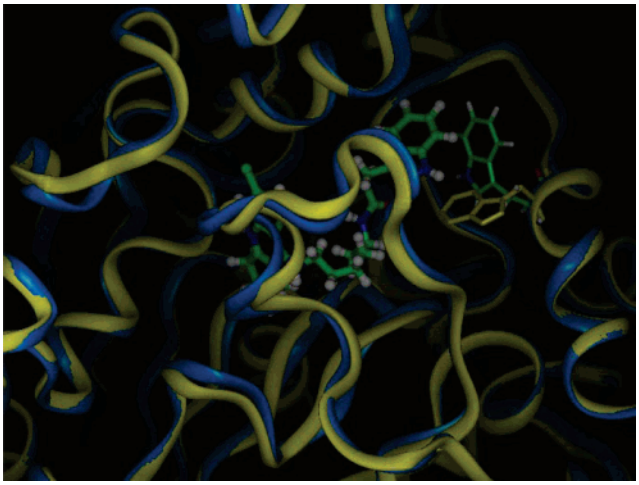

Figure 4. Superposition of the backbone of AChE in the X-ray crystallographic structure complexed with huprine X (PDB entry 1E66; yellow) and in a representative structure of the AChE complex with heterodimer **5** (blue). The inhibitor is represented as a colored ball-and-stick model, and the side chain of Trp279 is displayed using a stick model.

Finally, the indole ring is roughly stacked onto the aromatic ring of Trp279. Moreover, after the first nanosecond of the simulation, the NH group of the indole ring forms a water-mediated interaction with the hydroxyl oxygen of Tyr70 (average N···O distance: 5.18 Å). In this orientation, position 5 of the indole unit lies close to the backbone of Gly335 and to the side chain of Ile287 (average distances from C5 to Cα in Gly335 and Cβ in Ile287 ranging between 3.7 and 4.4 Å), which justifies the decrease in inhibitory activity observed upon inclusion of cyano and bromide substituents (see above and Table 1). Remarkably, there is a notable conformational rearrangement in the side chain of Trp279 (see Figure 4). Since the peripheral site region has been postulated to mediate the interaction of AChE with the Aβ nonamyloidogenic form,[17] it might be hypothesized that binding of compound **5** might have a significant effect in modulating the AChE-induced Aβ peptide fibrillogenesis.

AChE/BChE Selectivity. Recent evidence has shown that in AD patients with severe pathology, AChE is greatly reduced in specific brain regions, while BChE, which catalyzes the hydrolysis of a wide variety of choline esters (butyrylcholine, succinylcholine, and acetylcholine), noncholine esters, acyl amides, and aromatic amines, increases.[43] Therefore, to further characterize the pharmacological profile of the heterodimers, their selectivity to inhibit AChE vs BChE was determined.

The selectivity for BChE is generally small in the case of the 6-chlorotacrine substituted heterodimers **14**−**17** and **23**, it being much less pronounced than the effect due to the detachment of the chlorine atom in compounds **3** and **10**, which reflect and even enhance the larger binding affinity of tacrine for BChE. Particularly, **10** is around 700-fold more selective for BChE than tacrine. Remarkably, the AChE/BChE selectivity of compound **10** is reversed in its 6-chloro derivative

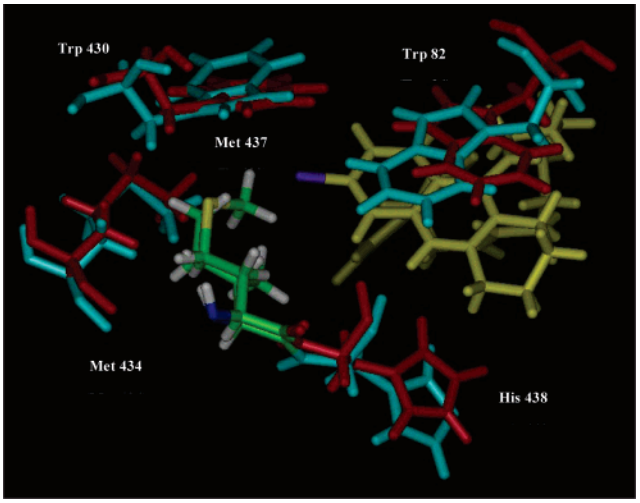

Figure 5. Representation of selected residues in the catalytic binding site of the MD-averaged structure of the complex between AChE (blue) and heterodimer **5** (yellow, but the chlorine atom is shown in magenta), and the superposed structure of BChE (PDB entry 1N5R; red). An atom-based color code is used to distinguish between Met437 in BChE and Ile439 in AChE. The numbering denotes the residues in BChE.

Table 3. Inhibition of Aβ_{1-40} Peptide Aggregation (with and without Human AChE) by Some Heterodimers and Reference Compounds

	with AChE		without AChE
compd	inhibition at 100 μM ± SEM (%)	IC_{50} ± SEM (μM)	inhibition at 100 μM ± SEM (%)
5	98 ± 2	2 ± 1	49 ± 7
6	96 ± 0	6 ± 2	65 ± 5
18	84 ± 1	7 ± 4	63 ± 10
20	99 ± 4	2 ± 0	63 ± 4
19	82 ± 1	15 ± 3	62 ± 14
propidium	82[a]	13 ± 0	46 ± 5
decamethonium	25[a]	nd[b]	0
donepezil	22[a]	nd[b]	0
tacrine	7[a]	nd[b]	0
edrophonium	0[a]	nd[b]	nd[b]
physostigmine	30[a]	nd[b]	nd[b]

[a] SD within 3% (data from ref 43). [b] nd = not determined.

(compound **11**), in agreement with the findings obtained for homodimeric tacrine inhibitors.[44] The influence of the chlorine atom on the AChE/BChE selectivity can be explained by the replacement of Ile439 in AChE by Met437 in BChE, as noted in the superposition (Figure 5) of the MD-averaged structure of the AChE−**5** complex to BChE (PDB entry 1N5R). Such a replacement eliminates the hydrophobic pocket that anchors the chlorine atom in AchE[39,40] and makes the terminal methyl group of Met437 in BChE to be around 1.1 Å closer to the chlorine atom, thus leading to steric hindrance with the 6-chlorotacrine unit.

Effects on the Aβ Aggregation. The heterodimers showing best AChE inhibitory potency (**5**, **6**, and **18**−**20**) were selected to assess their ability to inhibit Aβ_{1-40} peptide aggregation employing the thioflavin T fluorescence method and using propidium, a known inhibitor acting at the AChE peripheral site, as reference compound. Results showed that the heterodimers inhibited the Aβ peptide aggregation at 100 μM in a range varying from 49% to 63% (Table 3), they being at least as potent as propidium, which caused 46% inhibition. To further explore the dual action of these compounds, the capacity of **5**, **6**, and **18**−**20** to inhibit the AChE-induced Aβ_{1-40} peptide fibrillogenesis was examined employing the same thioflavin T-based fluorometric assay. Results are also shown in Table 3, where propidium and some other typical inhibitors of AChE have been used as reference compounds.[45] The most active compounds were **5** and **20**, followed by **6**, **18**, and **19**, the latter being around 2-, 3-, and 10-fold less active than the former compounds, respectively. With only the exception of heterodimer **19**, all of them were more active than the reference compound propidium, which is the most potent AChE-induced Aβ_{1-40} peptide antiaggregating drug reported so far (see Table 3 for comparison with commercially available AChE inhibitors). Clearly, these findings point out a potential disease-modifying action for this new family of dual AChE inhibitors.

Cell Viability. The cytotoxic effect of this new family of heterodimers was assayed in the human neuroblastoma cell line SH-SY5Y. For compounds **6**, **7**, and **11** only, toxicity was found at 10 μM (several orders of magnitude higher than the active concentration). For the rest of compounds we did not found any toxicity at this concentration. Therefore, we state that these new compounds possess a wide therapeutic safety range.

Conclusions

We have synthesized a series of indole−tacrine heterodimers as dual binding site AChE inhibitors. These compounds display high inhibitory potency against AChE (bovine and human) and, in general, are rather selective for AChE regarding BChE. More importantly, compounds **5**, **6**, and **18**−**20** inhibit the AChE-induced Aβ peptide aggregation in vitro, showing lower IC_{50} values than propidium, thus rendering new potent compounds acting as disease-modifying agents for the treatment of AD. In fact, preliminary in vivo studies in a transgenic mice overexpressing human APP (hAPP-(751)) suggest that this class of tacrine−indole heterodimers leads to a net reduction of Aβ peptide plaque load in the animals and an improvement in their cognitive functions.[46] This work is in progress and will be published. Taken together, all the preceding results suggest that the new dual binding AChE inhibitors have potential impact for the future therapeutic treatment of AD.

Experimental Section

Chemistry. All reagents were of commercial quality. All experiments involving water-sensitive compounds were carried out under nitrogen and scrupulously dry conditions, using anhydrous solvents purchased from Aldrich. Analytical thin-layer chromatography (TLC) was performed on aluminum sheets with precoated silica plates, 0.2 mm layer silica gel 60 F_{254} (Merck). Preparative centrifugal circular thin-layer chromatography (CCTLC) was performed on 20 cm diameter circular glass plates coated with a 1 mm layer of Kieselgel 60 PF_{254} (Merk), by using a Chromatotron, with the indicated solvent as eluent. Flash column chromatography was performed at medium pressure on silica gel 60 (particle size 0.040−0.063 mm, 230−240 mesh ASTM, Merck). ^{1}H NMR and ^{13}C NMR spectra were recorded with Mercury Plus Varian spectrometers operating at 400 and 50 MHz and using tetramethylsilane (TMS) as reference. Chemical shifts are reported in parts per million (ppm) relative to TMS. Elemental analyses were obtained in a LECO CHNS-932 apparatus. Analytical RP HPLC was performed on an Alliance 2605 (Waters) provided with a PDA2996 variable-wavelength detec-

tor and using an Xterra MS C18 column (4.6 mm × 150 mm), a Symmetry C18 column (2.1 mm × 150 mm), or an Atlantis DC18 3 μm (2.1 mm × 100 mm), depending on the case. Mixtures of 0.1% of formic acid in water (solvent A) and 0.1% of formic acid in CH_3CN (solvent B) were used as mobile phases.

General Procedure for the Synthesis of Indole−Tacrine Analogues 3−23. To a solution of the corresponding indole carboxylic acid **2a**−**i** derivative in anhydrous THF was added 1,1′-carbonyldiimidazol under N_2, and the resulting mixture was stirred for 4 h at room temperature. A solution of the corresponding 9-alkylaminotetrahydroacridine **1a**−**i** in THF was added, and the stirring was continued for a further 20 h. After evaporation of the solvent under reduced pressure, water was added and the resulting mixture was extracted with dichloromethane. The combined organic extracts were washed with saturated NaCl solution and dried with Na_2SO_4. Evaporation of the solvent under reduced pressure gave a residue that was purified by silica gel flash-column chromatography as indicated below for each case.

3-(1*H*-Indol-3-yl)-*N*-[5-(1,2,3,4-tetrahydroacridin-9-ylamino)pentyl]propionamide (3). Indole-3-propionic acid (**2a**) (63 mg, 0.33 mmol), anhydrous THF (3 mL), 1,1′-carbonyldiimidazol (57 mg, 0.35 mmol), and 9-(5-aminopentylamino)-1,2,3,4-tetrahydroacridine (**1a**) (100 mg, 0.35 mmol) were used to produce **3**. Purification: DCM/MeOH (3:1). Yellow foam (147 mg, 97%). RP HPLC (Atlantis DC18) t_R = 7.83 (8 min gradient from 95:5 to 0:100 A/B). ESI-MS *m/z* 455 [M + H]$^+$. Anal. ($C_{29}H_{34}N_4O\cdot H_2O$) C, H, N.

***N*-[5-(6-Chloro-1,2,3,4-tetrahydroacridin-9-ylamino)pentyl]-3-(1*H*-indol-3-yl)propionamide (4).** Indole-3-propionic acid (**2a**) (57 mg, 0.3 mmol), anhydrous THF (3 mL), 1,1′-carbonyldiimidazol (51 mg, 0.32 mmol), and 6-chloro-9-(5-aminopentylamino)-1,2,3,4-tetrahydroacridine (**1b**) (100 mg, 0.32 mmol) were used to produce **4**. Purification: DCM/MeOH (7:1). Yellow foam (121 mg, 83%). RP HPLC (Symmetry C18) t_R = 5.95 (10 min gradient from 100:0 to 0:100 A/B). ESI-MS *m/z* 489 [M + H]$^+$. Anal. ($C_{29}H_{33}ClN_4O$) C, H, N.

***N*-[5-(6-Chloro-1,2,3,4-tetrahydroacridin-9-ylamino)hexyl]-3-(1*H*-indol-3-yl)propionamide (5).** Indole-3-propionic acid (**2a**) (70 mg, 0.37 mmol), anhydrous THF (3 mL), 1,1′carbonyldiimidazole (63 mg, 0.39 mmol), and 6-chloro-9-(6-aminohexylamino)-1,2,3,4-tetrahydroacridine (**1c**) (131 mg, 0.39 mmol) were used to produce **5**. Purification: DCM/MeOH (50:1, 25:1, 20:1). Yellow foam (143 mg, 77%). RP HPLC (Symmetry C18) t_R = 5.43 (8 min from 95:5 to 0:100 A/B). ESI-MS *m/z* 503 [M + H]$^+$. Anal. ($C_{30}H_{35}ClN_4O\cdot 0.5H_2O$) C, H, N.

***N*-[7-(6-Chloro-1,2,3,4-tetrahydroacridin-9-ylamino)heptyl]-3-(1*H*-indol-3-yl)propionamide (6).** Indole-3-propionic acid (**2a**) (70 mg, 0.37 mmol), anhydrous THF (3 mL), 1,1′-carbonyldiimidazole (63 mg, 0.39 mmol), and 6-chloro-9-(7-aminoheptylamino)-1,2,3,4-tetrahydroacridine (**1d**) (135 mg, 0.39 mmol) were used to produce **6**. Purification: AcOEt/MeOH (50:1). Yellow foam (151 mg, 79%). RP HPLC (Symmetry C18) t_R = 5.60 (8 min from 95:5 to 0:100 A/B). ESI-MS *m/z* 517 [M + H]$^+$. Anal. ($C_{31}H_{37}ClN_4O\cdot 0.5H_2O$) C, H, N.

***N*-[8-(6-Chloro-1,2,3,4-tetrahydroacridin-9-ylamino)octyl]-3-(1*H*-indol-3-yl)propionamide (7).** Indole-3-propionic acid (**2a**) (70 mg, 0.37 mmol), anhydrous THF (3 mL), 1,1′-carbonyldiimidazole (63 mg, 0.39 mmol), and 6-chloro-9-(8-aminooctylamino)-1,2,3,4-tetrahydroacridine (**1e**) (140 mg, 0.39 mmol) were used to produce **7**. Purification: AcOEt/MeOH (50:1). Yellow syrup (104 mg, 53%). RP HPLC (Symmetry C18) t_R = 5.77 (8 min from 95:5 to 0:100 A/B). ESI-MS *m/z* 531 [M + H]$^+$. Anal. ($C_{32}H_{39}ClN_4O\cdot 0.5H_2O$) C, H, N.

***N*-[9-(6-Chloro-1,2,3,4-tetrahydroacridin-9-ylamino)nonyl]-3-(1*H*-indol-3-yl)propionamide (8).** Indole-3-propionic acid (**2a**) (28 mg, 0.15 mmol), anhydrous THF (3 mL), 1,1′-carbonyldiimidazole (25 mg, 0.15 mmol), and 6-chloro-9-(9-aminononylamino)-1,2,3,4-tetrahydroacridine (**1f**) (57 mg, 0.15 mmol) were used to produce **8**. Purification: DCM/MeOH (7:1).Yellow foam (10 mg, 14%). RP HPLC (Atlantis DC18) t_R = 8.90 (8 min gradient from 95:5 to 0:100 A/B and 2 min isocratic at 0:100 A/B). ESI-MS *m/z* 545 [M + H]$^+$. Anal. ($C_{33}H_{41}ClN_4O\cdot H_2O$) C, H, N.

***N*-[10-(6-Chloro-1,2,3,4-tetrahydroacridin-9-ylamino)decyl]-3-(1*H*-indol-3-yl)propionamide (9).** Indole-3-propionic acid (**2a**) (47 mg, 0.25 mmol), anhydrous THF (4 mL), 1,1′-carbonyldiimidazol (44 mg, 0.27 mmol), and 6-chloro-9-(10-aminodecylamino)-1,2,3,4-tetrahydroacridine (**1g**) (105 mg, 0.27 mmol) were used to produce **9**. Purification: DCM/MeOH (10:1). Yellow foam (21 mg, 19%). RP HPLC (Atlantis DC18) t_R = 9.18 (8 min gradient from 95:5 to 0:100 A/B and 2 min isocratic at 0:100 A/B). ESI-MS *m/z* 559 [M + H]$^+$. Anal. ($C_{34}H_{43}ClN_4O\cdot 2H_2O$) C, H, N.

***N*-(3-{[3-(1,2,3,4-Tetrahydroacridin-9-ylamino)propyl]methylamino}propyl)-3-(1*H*-indol-3-yl)propionamide (10).** Indole-3-propionic acid (**2a**) (56 mg, 0.29 mmol), anhydrous THF (4 mL), 1,1′carbonyldiimidazole (50 mg, 0.31 mmol), and N^1-[3-(1,2,3,4-tetrahydroacridin-9-ylamino)propyl]-N^1-methylpropane-1,3-diamine (**1h**) (100 mg, 0.31 mmol) were used to produce **10**. Purification: DCM/MeOH (20:1 + 0.1% NH_3, 10:1 + 0.2% NH_3, 10:1 + 0.4% NH_3). Yellow syrup (70 mg, 46%). RP HPLC (Symmetry C18) t_R = 3.98 (8 min gradient from 95:5 to 0:100 A/B). ESI-MS: *m/z* 498 [M + H]$^+$. Anal. ($C_{31}H_{39}N_5O\cdot H_2O$) C, H, N.

***N*-(3-{[3-(6-Chloro-1,2,3,4-tetrahydroacridin-9-ylamino)propyl]methylamino}propyl)-3-(1*H*-indol-3-yl)propionamide (11).** Indole-3-propionic acid (**2a**) (56 mg, 0.29 mmol), anhydrous THF (4 mL), 1,1′-carbonyldiimidazole (50 mg, 0.31 mmol), and N^1-[3-(6-chloro-1,2,3,4-tetrahydroacridin-9-ylamino)propyl]-N^1-methylpropane-1,3-diamine (**1i**) (100 mg, 0.31 mmol) were used to produce **11**. Purification: DCM/MeOH (20:1 + 0.1% NH_3, 10:1 + 0.2% NH_3, 10:1 + 0.4% NH_3). Yellow syrup (70 mg, 46%). RP HPLC (Atlantis DC18) t_R = 1.50 (8 min gradient from 95:5 to 0:100 A/B). ESI-MS: *m/z* 532 [M + H]$^+$. Anal. ($C_{31}H_{38}ClN_5O$) C, H, N.

***N*-[6-(6-Chloro-1,2,3,4-tetrahydroacridin-9-ylamino)hexyl]-3-(5-cyano-1*H*-indol-3-yl)propionamide (12).** 5-Cyanoindole-3-propionic acid (**2b**) (111 mg, 0.52 mmol),[35] anhydrous THF (10 mL), 1,1′-carbonyldiimidazol (84 mg, 0.52 mmol), and 6-chloro-9-(6-aminohexylamino)-1,2,3,4-tetrahydroacridine (**1c**) (164 mg, 0.49 mmol) were used to produce **12**. Purification: EtOAc/MeOH 50:1. Yellow syrup (60 mg 22%). RP HPLC (Symmetry C18) t_R = 5.33 (8 min from 95:5 to 0:100 A/B). ESI-MS: *m/z* 528 [M + H]$^+$. Anal. ($C_{31}H_{34}ClN_5O\cdot 1.5H_2O$) C, H, N.

***N*-[6-(6-Chloro-1,2,3,4-tetrahydroacridin-9-ylamino)hexyl]-3-(1*H*-indol-3-yl)acrylamide (13).** Indole-3-acrylic acid (**2c**) (88 mg, 0.47 mmol), anhydrous THF (6 mL), 1,1′-carbonyldiimidazole (76 mg, 0.47 mmol), and 6-chloro-9-(6-aminohexylamino)-1,2,3,4-tetrahydroacridine (**1c**) (150 mg, 0.45 mmol) were used to produce **13**. Purification: EtOAc/MeOH (100:1, 100:1 + 0.1% NH_3). Yellow foam (20 mg, 8%). RP HPLC (Symmetry C18) t_R = 5.46 (8 min from 95:5 to 0:100 A/B). ESI-MS: *m/z* 501 [M]$^+$. Anal. ($C_{30}H_{33}ClN_4O\cdot H_2O$) C, H, N.

1*H*-Indole-3-carboxylic Acid [5-(6-Chloro-1,2,3,4-tetrahydroacridin-9-ylamino)pentyl]amide (14). Indole-3-carboxylic acid (**2d**) (151 mg, 0.94 mmol), anhydrous THF (4 mL), 1,1′-carbonyldiimidazole (153 mg, 0.94 mmol), and 6-chloro-9-(5-aminopentylamino)-1,2,3,4-tetrahydroacridine (**1b**) (276 mg, 0.90 mmol) were used to produce **14**. Purification: EtOAc/MeOH 50:1. Yellow foam (198 mg, 52%). RP HPLC (Symmetry C18) t_R = 5.12 (8 min from 95:5 to 0:100 A/B). ESI-MS: *m/z* 461.07 [M]$^+$. Anal. ($C_{27}H_{29}ClN_4O\cdot H_2O$) C, H, N.

1*H*-Indole-3-carboxylic Acid [6-(6-Chloro-1,2,3,4-tetrahydroacridin-9-ylamino)hexyl]amide (15). Indole-3-carboxylic acid (**2d**) (153 mg, 0.95 mmol), anhydrous THF (10 mL), 1,1′-carbonyldiimidazole (154 mg, 0.95 mmol), and 6-chloro-9-(6-aminohexylamino)-1,2,3,4-tetrahydroacridine (**1c**) (300 mg, 0.90 mmol) were used to produce **15**. Purification: EtOAc/MeOH 50:1. Clear yellow foam (120 mg, 28%). RP HPLC (Symmetry C18) t_R = 5.32 (8 min from 95:5 to 0:100 A/B). ESI-MS: *m/z* 475 [M + H]$^+$. Anal. ($C_{28}H_{31}ClN_4O$) C, H, N.

1*H*-Indole-3-carboxylic Acid [7-(6-Chloro-1,2,3,4-tetrahydroacridin-9-ylamino)heptyl]amide (16). Indole-3-

carboxylic acid (**2d**) (147 mg, 0.91 mmol), anhydrous THF (10 mL), 1,1′-carbonyldiimidazole (147 mg, 0.91 mmol), and 6-chloro-9-(7-aminoheptylamino)-1,2,3,4-tetrahydroacridine (**1d**) (300 mg, 0.87 mmol). Purification: EtOAc/MeOH 50:1. Yellow foam (226 mg, 51%). RP HPLC (Symmetry C18) t_R = 5.49 (8 min from 95:5 to 0:100 A/B). ESI-MS: *m/z* 489 $[M + H]^+$. Anal. ($C_{29}H_{33}ClN_4O \cdot H_2O$) C, H, N.

1*H*-Indole-3-carboxylic Acid [8-(6-Chloro-1,2,3,4-tetrahydroacridin-9-ylamino)octyl]amide (17). Indole-3-carboxylic acid (**2d**) (92 mg, 0.57 mmol), anhydrous THF (3 mL), 1,1′-carbonyldiimidazol (92 mg, 0.57 mmol), and 6-chloro-9-(8-aminooctylamino)-1,2,3,4-tetrahydroacridine (**1e**) (196 mg, 0.54 mmol) were used to produce **17**. Purification: hexane/EtOAc (1:2 + 0.1% NH_3, 1:3 + 0.2% NH_3). Yellow foam (110 mg, 40%). RP HPLC (Symmetry C18) t_R = 5.67 (8 min from 95:5 to 0:100 A/B). ESI-MS: *m/z* 503 $[M + H]^+$. Anal. ($C_{30}H_{35}ClN_4O$) C, H, N.

***N*-[7-(6-Chloro-1,2,3,4-tetrahydroacridin-9-ylamino)heptyl]-2-(1*H*-indol-3-yl)acetamide (18).** Indole-3-acetic acid (**2e**) (1.10 g, 6.3 mmol), anhydrous THF (50 mL), 1,1′-carbonyldiimidazole (1.07 g, 6.6 mmol), and 6-chloro-9-(7-aminoheptylamino)-1,2,3,4-tetrahydroacridine (**1d**) (2.29 g, 6.6 mmol) were used to produce **18**. Purification: EtOAc/MeOH 50:1. Clear yellow foam (2.48 g, 80%). RP HPLC (Symmetry C18) t_R = 5.52 (8 min from 95:5 to 0:100 A/B). ESI-MS: *m/z* 503 $[M + H]^+$. Anal. ($C_{30}H_{35}ClN_4O \cdot H_2O$) C, H, N.

2-(5-Bromo-1*H*-indol-3-yl)-*N*-[7-(6-chloro-1,2,3,4-tetrahydroacridin-9-ylamino)heptyl]acetamide (19). 5-Bromoindole-3-acetic acid (**2f**) (155 mg, 0.61 mmol), anhydrous THF (10 mL), 1,1′-carbonyldiimidazol (99 mg, 0.61 mmol), and 6-chloro-9-(7-aminoheptylamino)-1,2,3,4-tetrahydroacridine (**1d**) (200 mg, 0.58 mmol) were used to produce **19**. Purification: EtOAc/MeOH 50:1. Clear yellow foam (185 mg, 54%). RP HPLC (Symmetry C18) t_R = 5.76 (8 min from 95:5 to 0:100 A/B). ESI-MS: *m/z* 581 $[M + 1, {}^{79}Br]^+$, 583 $[M + 1, {}^{81}Br]^+$. Anal. ($C_{30}H_{35}ClN_4O \cdot H_2O$) C, H, N.

***N*-[5-(6-Chloro-1,2,3,4-tetrahydroacridin-9-ylamino)pentyl]-4-(1*H*-indol-3-yl)butyramide (20).** Indole-3-butyric acid (**2g**) (134 mg, 0.66 mmol), anhydrous THF (10 mL), 1,1′-carbonyldiimidazole (107 mg, 0.66 mmol), and 6-chloro-9-(5-aminopentylamino)-1,2,3,4-tetrahydroacridine (**1b**) (200 mg, 0.63 mmol) were used to produce **20**. Purification: EtOAc/MeOH 100:1. Yellow foam (220 mg, 44%). RP HPLC (Symmetry C18) t_R = 5.43 (8 min from 95:5 to 0:100 A/B). ESI-MS: *m/z* 503 $[M + H]^+$. Anal. ($C_{30}H_{35}ClN_4O \cdot H_2O$) C, H, N.

***N*-[6-(6-Chloro-1,2,3,4-tetrahydroacridin-9-ylamino)hexyl]-4-(1*H*-indol-3-yl)butyramide (21).** Indole-3-butyric acid (**2g**) (134 mg, 0.66 mmol), anhydrous THF (8 mL), 1,1′-carbonyldiimidazol (107 mg, 0.66 mmol), and 6-chloro-9-(6-aminohexylamino)-1,2,3,4-tetrahydroacridine (**1c**) (200 mg, 0.63 mmol) were used to produce **21**. Purification: silica gel column chromatography using DCM/MeOH (20:1, 20:1 + 0.01% NH_3). Yellow syrup (163 mg, 48%). RP HPLC (Symmetry C18) t_R = 5.32 (8 min from 95:5 to 0:100 A/B). ESI-MS: *m/z* $[M + H]^+$ 517. Anal. ($C_{31}H_{37}ClN_4O \cdot H_2O$) C, H, N.

1*H*-Methylindole-3-carboxylic Acid [7-(6-Chloro-1,2,3,4-tetrahydroacridin-9-ylamino)heptyl]amide (22). 1-Methylindole-3-carboxylic acid (**2h**) (214 mg, 1.22 mmol), anhydrous THF (20 mL), 1,1′-carbonyldiimidazole (197 mg, 1.22 mmol), and 6-chloro-9-(7-aminoheptylamino)-1,2,3,4-tetrahydroacridine (**1d**) (400 mg, 1.16 mmol) were used to produce **22**. Purification: EtOAc/MeOH 50:1. Yellow foam (141 mg, 23%). RP HPLC (Symmetry C18) t_R = 5.70 (8 min from 95:5 to 0:100 A/B). ESI-MS: *m/z* 503 $[M + H]^+$. Anal. ($C_{30}H_{35}ClN_4O \cdot H_2O$) C, H, N.

1*H*-Indazole-3-carboxylic Acid [7-(6-Chloro-1,2,3,4-tetrahydroacridin-9-ylamino)heptyl]amide (23). Indazole-3-carboxylic acid (**2h**) (187 mg, 1.15 mmol), anhydrous THF (5 mL), 1,1′-carbonyldiimidazol (162 mg, 1.20 mmol), and 6-chloro-9-(7-aminoheptylamino)-1,2,3,4-tetrahydroacridine (**1d**) (345 mg, 1.15 mmol) were used to produce **23**. Purification: EtOAc/MeOH 50:1. Yellow syrup (79 mg, 13%). RP HPLC (Symmetry C18) t_R = 5.58 (8 min from 95:5 to 0:100 A/B). ESI-MS: *m/z* 490 $[M + H]^+$. Anal. ($C_{28}H_{32}ClN_5O$) C, H, N.

Synthesis of Intermediate Carbonic Acid 2-(1*H*-Indol-3-yl)ethyl Ester 4-Nitrophenyl Ester (26). To a solution of 2-(1*H*-indol-3-yl)ethanol (**24**) (1600 mg, 9.92 mmol) in *N*-methylmorpholine (2000 mg, 19.84 mmol) was added *p*-nitrophenyl chloroformate (**25**) (4000 mg, 19.84 mmol), and the mixture was stirred for 24 h at room temperature. Water was added, and the mixture was extracted with dichloromethane. Evaporation of the solvent gave a residue that was purified by silica gel column chromatography using a mixture of DCM/hexane (3:1) as eluent to produce the title compound **26** (1034 mg, 32%) as a yellow solid. ESI-MS 327 *m/z* $[M + H]^+$.

General Synthesis of Carbamate Derivatives 27−29. To a solution of the carbonic acid 2-(1*H*-indol-3-yl)ethyl ester 4-nitrophenyl ester (**26**) in MeOH was added a solution of the corresponding alkylaminotetrahydroacridine in DMF, in the presence of DMAP, and the resulting mixture was stirred for 24 h at room temperature. After evaporation of the solvent under reduced pressure, water was added and the resulting mixture was extracted with dichloromethane. The combined organic extracts were washed with saturated NaCl solution and filtered, and the solvent was evaporated to give a residue that was purified by silica gel column chromatography as indicated below for each case.

[5-(6-Chloro-1,2,3,4-tetrahydroacridin-9-ylamino)pentyl]carbamic Acid 2-(1*H*-Indol-3-yl)ethyl Ester (27). N^1-(6-Chloro-1,2,3,4-tetrahydroacridin-9-yl)pentane-1,5-diamine (**1b**) (500 mg, 1.58 mmol), carbonic acid 2-(1*H*-indol-3-yl)ethyl ester 4-nitrophenyl ester (**26**) (260 mg, 0.79 mmol), and DMAP (1930 mg, 1.58 mmol) were used to produce **27**. Purification: DCM/MeOH (7:0.5). Yellow syrup (126 mg, 32%). RP HPLC (Atlantis DC18) t_R = 8.60 (8 min gradient from 95:5 to 0:100 A/B and 2 min isocratic at 0:100 A/B). ESI-MS: *m/z* 505.1 $[M + H]^+$. Anal. ($C_{29}H_{33}ClN_4O_2 \cdot H_2O$) C, H, N.

[6-(6-Chloro-1,2,3,4-tetrahydroacridin-9-ylamino)hexyl]carbamic Acid 2-(1*H*-Indol-3-yl)ethyl Ester (28). N^1-(6-Chloro-1,2,3,4-tetrahydroacridin-9-yl)hexane-1,6-diamine (**1c**) (610 mg, 1.84 mmol), carbonic acid 2-(1*H*-indol-3-yl)ethyl ester 4-nitrophenyl ester (**26**) (300 mg, 0.92 mmol), and DMAP (225 mg, 1.84 mmol) were used to produce **28**. Purification: DCM/MeOH (7:0.5). Amber syrup (100 mg, 21%). RP HPLC (Atlantis DC18) t_R = 8.70 (8 min gradient from 95:5 to 0:100 A/B and 2 min isocratic at 0:100 A/B). ESI-MS: *m/z* 519.2 $[M + H]^+$. Anal. ($C_{30}H_{35}ClN_4O_2 \cdot 0.5H_2O$) C, H, N.

[7-(6-Chloro-1,2,3,4-tetrahydroacridin-9-ylamino)heptyl]carbamic Acid 2-*(1H*-Indol-3-yl)ethyl Ester (29). N^1-(6-Chloro-1,2,3,4-tetrahydroacridin-9-yl)heptane-1,7-diamine (**1d**) (344 mg, 1.0 mmol), carbonic acid 2-(1*H*-indol-3-yl)ethyl ester 4-nitrophenyl ester (**26**) (166 mg, 0.5 mmol), and DMAP (122 mg, 1.0 mmol) were used to produce **29**. Purification: DCM/MeOH (7:0.5). Amber syrup (70 mg, 40%). RP HPLC (Atlantis DC18) t_R = 8.90 (8 min gradient from 95:5 to 0:100 A/B and 2 min isocratic at 0:100 A/B). ESI-MS: *m/z* 533.1 $[M + H]^+$. Anal. ($C_{31}H_{37}ClN_4O_2 \cdot 0.5H_2O$) C, H, N.

Biochemical Methods. In Vitro AChE Inhibition Assay. Inhibitory activity against AChE was evaluated at 30 °C by the colorimetric method reported by Ellman et al.[39] The assay solution consisted of 0.1 M phosphate buffer, pH 8, 0.3 mM 5,5′-dithiobis(2-nitrobenzoic acid) (DTNB, Ellman's reagent), 0.02 units of AChE (Sigma Chemical Co. from bovine erythrocytes or human brain), and 0.5 mM acetylthiocholine iodide as the substrate of the enzymatic reaction. Compounds tested were added to the assay solution and preincubated with the enzyme for 10 min at 30 °C. After that period, the substrate was added. The absorbance changes at 405 nm were recorded for 5 min with a microplate reader Digiscan 340T, the reaction rates were compared, and the percent inhibition due to the presence of the test compounds was calculated. The compound concentration producing 50% of AChE inhibition (IC_{50}) was determined for each compound. The sigmoidal dose response curves have been fit by nonlinear regression (GraphPad Prism 4 software). The experimental uncertainties were calculated as 95% confidence interval.

In Vitro BChE Inhibition Assay. BChE inhibitory activity was evaluated at 30 °C by the colorimetric method reported by Ellman et al.[39] The assay solution consisted of 0.01 units of BChE (Sigma Chemical Co. from human serum), 0.1 M sodium phosphate buffer, pH 8, 0.3 mM 5,5'-dithiobis(2-nitrobenzoic acid) (DTNB, Ellman's reagent), and 0.5 mM butyrylthiocholine iodide as the substrate of the enzymatic reaction. Enzyme activity was determined by measuring the absorbance at 405 nm during 5 min with a microplate reader Digiscan 340T. The tested compounds were preincubated with the enzyme for 10 min at 30 °C before starting the reaction by adding the substrate. The reaction rate was calculated with at least triplicate measurements. The IC_{50} is defined as the concentration of compounds that reduces by 50% the enzymatic activity with respect to that without inhibitors. The sigmoidal dose response curves have been fit by nonlinear regression (GraphPad Prism 4 software). The experimental uncertainties were calculated as 95% confidence interval.

Inhibition of β-Amyloid Peptide Aggregation Assay. Thioflavin T-Based Fluorometric Assay. Aβ peptide (1−40), lyophilized from HFIP solution (rPeptide, GA), was dissolved in DMSO to obtain a 2.3 mM solution. Aliquots of Aβ in DMSO were then incubated in constant rotation for 24 h at room temperature in 0.215 M sodium phosphate buffer (pH 8.0) at a final Aβ concentration of 10 μM in the presence or absence of compounds or propidium at 100 μM, used as reference. To quantify amyloid fibril formation, the thioflavin T fluorescence method was used. Analyses were performed with a Fluostar Optima plate reader (BMG). Fluorescence was measured at 450 nm (λ excitation) and 485 nm (λ emission). To determine amyloid fibril formation, after incubation, the solutions containing Aβ or Aβ plus AChE inhibitors were added to 50 mM glycine−NaOH buffer, pH 8.5, containing 3 μM thioflavin T in a final volume of 150 μL. Each assay was run in triplicate. The fluorescence intensities were recorded, and the percent aggregation was calculated by the following expression: $100 - (IF_i/IF_o \times 100)$ where IF_i and IF_o are the fluorescence intensities obtained for Aβ in the presence and in the absence of inhibitor, respectively, after subtracting the fluorescence of respective blanks (method adapted from ref 45).

Inhibition of AChE-Induced β-Amyloid Peptide Aggregation Assay. Thioflavin T-Based Fluorometric Assay. Aliquots of 2 μL Aβ(1−40) peptide (Bachem AG, Bubendorf, Switzerland), lyophilized from 2 mg mL^{-1} HFIP solution and dissolved in DMSO, were incubated for 24 h at room temperature in 0.215 M sodium phosphate buffer (pH 8.0) at a final concentration of 230 μM. For co-incubation experiments, aliquots (16 μL) of human recombinant AChE (final concentration of 2.30 μM, Aβ/AChE molar ratio of 100:1) and AChE in the presence of 2 μL of the tested inhibitors were added. Blanks containing Aβ, AChE, and Aβ plus inhibitors at various concentrations in 0.215 M sodium phosphate buffer (pH 8.0) were prepared. The final volume of each vial was 20 μL. Each assay was run in duplicate. Inhibitor stock solutions were prepared (c = 1.0 or 0.5 mM) and diluted in methanol. To quantify amyloid fibril formation, the thioflavin T fluorescence method is then applied.[47−49]

Analyses were performed with a Jasco spectrofluorimeter FP-750 using a 3 mL quartz cell. After incubation, the samples containing Aβ, Aβ plus AChE, or Aβ plus AChE in the presence of inhibitors were diluted with 50 mM glycine−NaOH buffer (pH 8.5) containing 1.5 μM thioflavin T to a final volume of 2.0 mL. Fluorescence was monitored with excitation at 446 nm and emission at 490 nm. A time scan of fluorescence is performed, and the intensity values reached at the plateau (around 300 s) are averaged after subtracting the background fluorescence from 1.5 μM thioflavin T and AChE.

The fluorescence intensities were compared, and the percentage of inhibition due to the presence of the tested compounds was calculated. The percent inhibition of the AChE-induced aggregation due to the presence of increasing concentrations of the inhibitor was calculated by the following expression: $100 - (IF_i/IF_o \times 100)$ where IF_i and IF_o are the fluorescence intensities obtained for Aβ plus AChE in the presence and in the absence of inhibitor, respectively, after subtracting the fluorescence of respective blanks. Inhibition curves were obtained for each compound by plotting the percent inhibition versus the logarithm of inhibitor concentration in the assay sample. The linear regression parameters were then determined and the IC_{50} was extrapolated, when possible (Microcal Origin, version 3.5, Microcal Software Inc.).

Cytotoxicity. The cytotoxicity effect of the synthesized compounds was studied in the human neuroblastoma cell line SH-SY5Y. These cells were cultured in 96-well plates in minimum essential medium and Ham's F12 medium, supplemented with 10% fetal bovine serum, 1% glutamine, and 1% penicillin/streptomycin, and grown in a 5% CO_2 humidified incubator at 37 °C. Cells were plated at 10^4 cells for each well at least 48 h before the toxicity measurements. Cells were exposed for 24 h to the compound at different concentrations, and quantitative assessment of cell death was made by measurement of the intracellular enzyme lactate dehydrogenase (LDH) (cytotoxicity detection kit, Roche). The quantity of LDH was evaluated in a microplate reader, Anthos 2010, at 492 nm (λ excitation) and 620 nm (λ emission). Controls were taken as having 100% viability.

Molecular modeling methods. Setup of the Model. The simulation system was defined following the protocol used in our previous studies on AChE−ligand complexes,[41,50] which is briefly summarized here. The simulation system was based on the X-ray crystallographic structures of the AChE complexes with tacrine (PDB entry 1ACJ),[51] huprine Y (1E66),[42] and donepezil (1EVE),[52] which were used as templates to position the 6-chlorotacrine unit in the catalytic binding site, the linker along the gorge, and the indole unit in the peripheral binding site. The enzyme was modeled in its physiologically active form with neutral His440 and deprotonated Glu327, which form together with Ser200 the catalytic triad. The standard ionization state at neutral pH was considered for the rest of the ionizable residues with the exception of Asp392 and Glu443, which were neutral, and His471, which was protonated, according to previous numerical titration studies.[53] Finally, Phe330 was replaced by Tyr to reflect the binding site sequence in bovine AChE. According to the basicity of the quinoline ring,[54] the heterodimer was protonated at the tacrine ring. The orientation of the methylene side chain with regard to tacrine was determined by means of geometry optimizations performed at the MP2/6-31G(d) level using Gaussian 03.[55] With regard to the indole moiety, two different starting orientations were initially chosen. In both cases the indole ring was stacked against Trp279, though they differed by a 180° rotation around the bond linking the indole unit to the methylene side chain of the linker. The system was hydrated by centering a sphere of 40 Å of TIP3P[56] water molecules at the inhibitor, paying attention to filling the position of the crystallographic waters inside the binding cavity. The parm98 file of the AMBER force field[57] was used to describe the enzyme. For the inhibitor, the charge distribution of tacrine, linker, and indole units was determined from fitting to the HF/6-31G(d) electrostatic potential using the RESP procedure,[58] and the van der Waals parameters were taken from those defined for related atoms in the AMBER force field. The final model system was partitioned into a mobile region and a rigid region. The former included the inhibitor, all the protein residues containing at least one atom within 15 Å from the inhibitor, and all the water molecules, while the rest of atoms defined the rigid part.

Molecular Dynamics Simulation. Starting from the two models of the inhibitor bound to the enzyme (differing in the orientation of the indole ring), the system was energy-minimized and equilibrated using the AMBER program.[59] First, all hydrogen atoms were minimized for 2000 steps of steepest descent. Next, the positions of water molecules were relaxed for 5000 steps of steepest descent plus 3000 steps of conjugate gradient. At this point, the rigid part of the system was kept frozen and the thermalization of the mobile part was started by running four 10 ps molecular dynamics (MD) simulations to increase the temperature to 298 K. Subse-

quently, a 6 ns MD simulation was carried out. Only one of the two simulations provided a stable trajectory, as noted in a small positional root-mean-square deviation (around 0.7 Å for the backbone atoms in the mobile region with regard to the crystallographic structure) and favorable contacts with the enzyme (see text). The characterization of the structural features that mediate the binding of compound **5** to the enzyme was determined by averaging the geometrical parameters for the snapshots (saved every picosecond) sampled along the last 2 ns of the MD simulation.

Supporting Information Available: Elemental analysis data for **3**−**23** and **27**−**29** and ^{1}H and ^{13}C NMR data for **3**−**23** and **26**−**29**. This material is available free of charge via the Internet at http://pubs.acs.org.

References

(1) Walsh, D. M.; Selkoe D. J. Deciphering the molecular basis of memory failure in Alzheimer's disease. *Neuron* **2004**, *44*, 181−193.

(2) Selkoe, D. J. Alzheimer's disease: genes, proteins and therapy. *Physiol. Rev*. **2001**, *81*, 741−766.

(3) Dekoski, S. T. Pathology and pathways of Alzheimer's disease with an update on new development and treatment. *J. Am. Geriatr. Soc*. **2003**, *51*, 314−320.

(4) Tariot P. N.; Federoff, H. J. Current treatment for Alzheimer's disease and future prospects. *Alzheimer Dis. Assoc. Disord*. **2003**, *17*, 105−113.

(5) Kurz, A. The therapeutical potential of tacrine. *J. Neural. Transm., Suppl*. **1998**, *54*, 295−299.

(6) Sugimoto, H. Donepezil hydrochloride: A treatment drug for Alzheimer's disease. *Chem. Rec.* **2001**, *1*, 63−73.

(7) Jann, M. W. Rivastigmine, a new-generation cholinesterase inhibitor for the treatment of Alzheimer's disease. *Pharmacotherapy* **2000**, *20*, 1−12.

(8) Zarotsky, V.; Sramek, J. J.; Cutler, N. R. Galantamine hydrobromide: an agent for Alzheimer's disease. *Am. J. Health-Syst. Pharm*. **2003**, *60*, 446−452.

(9) Soreq, H.; Seidman, S. Acetylcholinesterase: new roles for an old actor. *Nat. Rev. Neurosci.* **2001**, *2*, 8−17.

(10) Johnson, G.; Moore, S. W. The adhesion function on acetylcholinesterase is located at the peripheral anionic site. *Biochem. Biophys. Res. Commun.* **1999**, *258*, 758−762.

(11) Giacobini, E. Cholinesterases: New roles in brain function and in Alzheimer's disease. *Neurochem. Res.* **2003**, *28*, 515−522.

(12) Muñoz, F. J.; Aldunate, R.; Inestrosa, N. C. Peripheral binding site is involved in the neurotrophic activity of acetylcholinesterase. *NeuroReport* **1999**, *26*, 3621−3625.

(13) Sharma, K. V.; Koenigsberger, C.; Brimijoin, S.; Gigbee, J. W. Direct evidence for an adhesive function in the noncholinergic role of acetylcholinesterase in neurite outgrowth. *J Neurosci. Res.* **2001**, *63*, 165−175.

(14) Blasina, M. F.; Faria, A. C.; Gardino, P. F.; Hokoc, J. N.; Almeida, O. M.; de Mello, F. G.; Arruti, C.; Dajas, F. Evidence of noncholinergic function of acetylcholinesterase during development of chicken retina as shown by fasciculin. *Cell Tissue Res.* **2000**, *299*, 173−184.

(15) Inestrosa, N. C.; Alarcón, R. Molecular interactions of acetylcholinesterase with senile plaques. *J. Physiol. (Paris)* **1998**, *92*, 341−344.

(16) Inestrosa, N. C.; Alvarez, A.; Calderon, F. Acetylcholinesterase is a senile plaque component that promotes assembly of amyloid beta-peptide into Alzheimer's filaments. *Mol. Psychiatry* **1996**, *1*, 359−361.

(17) De Ferrari, G. V.; Canales, M. A.; Shin, I.; Weiner, L. M.; Silman, I.; Inestrosa, N. C. A structural motif of acetylcholinesterase that promotes amyloid β-peptide fibril formation. *Biochemistry* **2001**, *40*, 10447−10457.

(18) Bartolini, M.; Bertucci, C.; Cavrini, V.; Andrisano, V. β-Amyloid aggregation induced by human acetylcholinesterase: inhibition studies. *Biochem. Pharmacol*. **2003**, *65*, 407−416.

(19) Pang, Y. P.; Quiram, P.; Jelacic, T.; Hong, F.; Brimijoin, S. Highly potent, selective, and low cost bis-tetrahydroaminoacrine inhibitors of acetylcholinesterase. *J. Biol. Chem.* **1996**, *271*, 23646−23649.

(20) Castro, A.; Martínez, A. Peripheral and dual binding site acetylcholinesterase inhibitors: Implications in the treatment of Alzheimer's disease. *Mini-Rev. Med. Chem.* **2001**, *1*, 267−272.

(21) Tumiatti, V.; Andrisano, V.; Banzi, R.; Bartolini, M.; Rosini, M.; Melchiorre, C. Structure activity relationships of acetylcholinesterase non-covalent inhibitors based on a polyamine backbone. 3. Effect of replacing the inner polymethylene chain with cyclic moieties. *J. Med. Chem.* **2004**, *47*, 6490−6498.

(22) Pang, Y. P.; Kollmeyer, T. M.; Hong, F.; Lee, J. C.; Hammond, P. I.; Haugabouk, S. P.; Brimijoin, S. Rational design of alkylene-linked bis-pyridiniumaldoximes as improved acetylcholinesterase reactivators. *Chem. Biol*. **2003**, *10*, 491−502.

(23) Piazzi, L.; Rampa, A.; Bisi, A.; Gobbi, S.; Belluti, F.; Cavalli, A.; Bartolini, M.; Andrisano, V.; Valenti, P.; Recanatini, M. 3-(4-[[Benzyl(methyl)amino]methyl]phenyl)-6,7-dimethoxy-2*H*-2-chromenone (AP2238) inhibits both acetylcholinesterase and acetylcholinesterase-induced β-amyloid aggregation: a dual function lead for Alzheimer's disease therapy. *J. Med. Chem.* **2003**, *46*, 2279−2282.

(24) Dorronsoro, I.; Castro, A.; Martínez, A. Peripheral and dual-binding site acetylcholinesterase inhibitors as neurodegenerative disease modifying agents. *Expert Opin. Ther. Pat.* **2003**, *13*, 1725−173.

(25) Martínez, A.; Fernández, E.; Castro, A.; Conde, S.; Rodríguez-Franco, M. I.; Baños, J. E.; Badía, A. *N*-Benzylpiperidine derivatives of 1,2,4-thiadiazolidinone as new acetylcholinesterase inhibitors. *Eur. J. Med. Chem.* **2000**, *35*, 913−919.

(26) Castro, A.; Hernández, L.; Dorronsoro, I.; Sáenz, P.; Pérez, C.; Kalko, S.; Orozco, M.; Luque, F. J.; Martínez, A. Synthesis, biological evaluation and modelling studies of dual binding AChE inhibitors. *Med. Chem. Res.* **2002**, *11*, 219−237.

(27) Dorronsoro, I.; Alonso, D.; Castro, A.; García-Palomero, E.; del Monte, M.; Martínez, A. Synthesis and biological evaluation of tacrine−thiadiazolidinone hybrids as dual acetylcholinesterase inhibitors. *Arch. Pharm. Pharm. Res* **2005**, *338*, 18−23.

(28) Martínez, A.; Dorronsoro, I.; Rubio, L.; Alonso, D.; Fuertes, A.; Morales-Alcelay, S.; Del Monte, M.; García-Palomero, E.; Usán, P.; De Austria, C.; Medina, M.; Muñoz, P. Tacrine derivatives as inhibitors of acetylcholinesterase. WO 2005/005413, 2005.

(29) Savini, L.; Gaeta, A.; Fattorusso, C.; Catalanotti, B.; Campiani, G.; Chiasserini, L.; Pellerano, C.; Novellino, E.; McKissic, D.; Saxena, A. Specific target of acetylcholinesterase and butyrylcholinesterase recognition sites. Rational design of novel, selective, and highly potent cholinesterase inhibitors. *J. Med. Chem.* **2003**, *46* (1), 1−4.

(30) Carlier, P. R.; Chow, E. S. H.; Han, Y.; Liu, J.; El Yazla, J.; Pang, Y. P. Heterodimeric tacrine-based acetylcholinesterase inhibitors: investigating ligand−peripheral site interactiones. *J. Med. Chem.* **1999**, *42*, 4225−4231.

(31) Rosini, M.; Andrisano, V.; Bartolini, M.; Bolognesi, M.; Hrelia, P.; Minarini, A.; Tarozzi, A.; Melchiorre, C. Rational Approach To Discover Multipotent Anti-Alzheimer Drugs. *J. Med. Chem.* **2005**, *48* (2), 360−363.

(32) Recanatini, M.; Cavalli, A.; Belluti, F.; Piazzi, L.; Rampa, A.; Bisi, A.; Gobbi, S.; Valenti, P.; Andrisano, V.; Bartolini, M.; Cavrini, V. SAR of 9-amino-1,2,3,4-tetrahydroacrydine-based acetylcholinesterase inhibitors synthesis, enzyme inhibitory activity, QSAR and structure-based COMFA of tacrine analogues. *J. Med. Chem.* **2000**, *43*, 2007−2018.

(33) Sippl, W.; Holtje, H. D. Structure-based 3D-QSAR−merging the accuracy of structure-based alignments with the computational efficiency of ligand-based methods. *J. Mol. Struct.: THEOCHEM* **2000**, *503*, 31−50.

(34) Morzyc-Ociepa, B.; Michaska, D.; Petraszco, A. Structures and vibrational structures of indole carboxylic acids. Part I. Indole-2-carboxylic acid. *J. Mol. Struct.* **2004**, *688*, 79−86.

(35) Ming-Kuan, H. U.; Jiajiu, S. Tacrine derivatives for treating Alzheimer's disease. WO01/17529, 2001.

(36) Padwa, A.; Harring, S. R.; Hertzog, D. L.; Nadlet, W. R. Cycloaddition chemistry of anhydro-4-hydroxy-1,3-thiazolium hydroxides for the synthesis of heterocycles. *Synthesis* **1994**, *9*, 993−1004.

(37) Agarwal, A.; Jalluri, R. K.; DeWitt Blanton, C.; Will Taylor, E. A new synthesis of the potent 5-HT$_1$ receptor ligand, 5-carboxyamidotryptamine *Synth. Commun*. **1993**, *23* (8), 1101−1110.

(38) Dressman, B. A.; Spangle, L. A.; Kaldor, S. W. Solid phase synthesis of hydantoins using a carbamate linker and a novel cyclization/cleavage step. *Tetrahedron Lett.* **1996**, *7*, 937−940.

(39) Ellman, G. L.; Courtney, K. D.; Andres, B.; Featherstone, R. M. A new and rapid colorimetric determination of acetylcholinesterase activity. *Biochem. Pharmacol*. **1961**, *7*, 88−95.

(40) Barril, X.; Kalko, S. G.; Orozco, M.; Luque, F. J. Rational design of reversible acetylcholinesterase inhibitors. *Mini-Rev. Med. Chem*. **2002**, *2*, 27−36.

(41) Camps, P.; El Achab, R.; Morral, J.; Muñoz-Torrero, D.; Badia, A.; Baños, J. E.; Vivas, N. M.; Barril, X.; Orozco, M.; Luque, F. J. New tacrine−huperzine A hybrids (huprines): highly potent tight-binding acetylcholinesterase inhibitors of interest for the treatment of Alzheimer's disease. *J. Med. Chem*. **2000**, *43*, 4657−4666.

(42) Dvir, H.; Wong, D. M.; Harel, M.; Barril, X.; Orozco, M.; Luque, F. J.; Muñoz-Torrero, D.; Camps, P.; Rosenberry, T. L.; Silman, I.; Sussman, J. L. 3D structure of *Torpedo californica* acetylcholinesterase complexed with huprine X at 2.1 Å resolution: Kinetic and molecular dynamics correlates. *Biochemistry* **2002**, *41*, 2970−2981.

(43) Greig, N. H.; Lahiri, D. K.; Sambamurti, K. Butyrylcholinesterase: an important new target in Alzheimer's disease therapy. *Int. Psychogeriatr*. **2002**, *14* (Suppl. 1), 77−91.
(44) Hu, M.-K.; Wu, L.-J.; Hsiao, G.; Yen, M.-H. Homodimeric tacrine congeners as acetylcholinesterase inhibitors. *J. Med. Chem*. **2002**, *45*, 2277−2282.
(45) Bartolini, M.; Bertucci, C.; Cavrini, V.; Andrisano, V. β-amyloid aggregation induced by human acetylcholinesterase: inhibiton studies *Biochem. Pharmacol*. **2003**, *65*, 407−416.
(46) Outcomes of this study recently presented in the 5th Neurobiology of Aging Conference in San Diego, CA, October 21−27, 2004.
(47) LeVine, H. Thioflavine T interaction with synthetic Alzheimer's disease beta-amyloid peptides: detection of amyloid aggregation in solution. *Protein Sci*. **1993**, *2*, 404−410.
(48) Naiki, H.; Higuchi, K.; Nakakuki, K.; Takeda, T. Kinetic analysis of amyloid fibril polymerization in vitro. *Lab. Invest*. **1991**, *65*, 104−110.
(49) LeVine, H., 3rd; Scholten, J. D. Screening for pharmacologic inhibitors of amyloid fibril formation. *Methods Enzymol*. **1999**, *309*, 467−476.
(50) Barril, X.; Orozco, M.; Luque, F. J. Predicting relative binding free energies of tacrine−huperzine A hybrids as inhibitors of acetylcholinesterase. *J. Med. Chem*. **1999**, *42*, 5110−5119.
(51) Sussman, J. L.; Harel, M.; Frolow, F.; Oefner, C.; Goldman, A.; Toker, L.; Silman, I. Atomic structure of acetylcholinesterase from *Torpedo californica*: a prototypic acetylcholine-binding protein. *Science* **1991**, *253*, 872−879.
(52) Kryger, G.; Silman, I.; Sussman, J. L. Structure of acetylcholinesterase complexed with E2020 (Aricept): Implications for the design of new anti-Alzheimer drugs. *Structure* **1999**, *7*, 297−307.
(53) Wlodek, S. T.; Antosiewicz, J.; McCammon, J. A.; Straatsma, T. P.; Gilson, M. K.; Briggs, M. J.; Humblet, C.; Sussman, J. L. Binding of tacrine and 6-chlorotacrine by acetylcholineterase. *Biopolymers* **1996**, *38*, 109−117.
(54) Foye, W. O.; Lemke, T. L.; Williams, D. A. *Principles of Medicinal Chemistry*, 4th ed.; Williams and Wilkins: Media, PA, 1995; Appendix Table A-1.
(55) Frisch, M. J.; Trucks, G. W.; Schlegel, H. B.; Scuseria, G. E.; Robb, M. A.; Cheeseman, J. R.; Montgomery, J. A., Jr.; Vreven, T.; Kudin, K. N.; Burant, J. C.; Millam, J. M.; Iyengar, S. S.; Tomasi, J.; Barone, V.; Mennucci, B.; Cossi, M.; Scalmani, G.; Rega, N.; Petersson, G. A.; Nakatsuji, H.; Hada, M.; Ehara, M.; Toyota, K.; Fukuda, R.; Hasegawa, J.; Ishida, M.; Nakajima, T.; Honda, Y.; Kitao, O.; Nakai, H.; Klene, M.; Li, X.; Knox, J. E.; Hratchian, H. P.; Cross, J. B.; Adamo, C.; Jaramillo, J.; Gomperts, R.; Stratmann, R. E.; Yazyev, O.; Austin, A. J.; Cammi, R.; Pomelli, C.; Ochterski, J. W.; Ayala, P. Y.; Morokuma, K.; Voth, G. A.; Salvador, P.; Dannenberg, J. J.; Zakrzewski, V. G.; Dapprich, S.; Daniels, A. D.; Strain, M. C.; Farkas, O.; Malick, D. K.; Rabuck, A. D.; Raghavachari, K.; Foresman, J. B.; Ortiz, J. V.; Cui, Q.; Baboul, A. G.; Clifford, S.; Cioslowski, J.; Stefanov, B. B.; Liu, G.; Liashenko, A.; Piskorz, P.; Komaromi, I.; Martin, R. L.; Fox, D. J.; Keith, T.; Al-Laham, M. A.; Peng, C. Y.; Nanayakkara, A.; Challacombe, M.; Gill, P. M. W.; Johnson, B.; Chen, W.; Wong, M. W.; Gonzalez, C.; Pople, J. A. *Gaussian 03*, revision B.04; Gaussian, Inc.: Pittsburgh, PA, 2003.
(56) Jorgensen, W. L.; Chandrasekhar, J.; Madura, J. D.; Impey, R. W.; Klein, M. L. Comparison of simple potential functions for simulating liquid water. *J. Chem. Phys*. **1983**, *79*, 926−935.
(57) Cornell, W. D.; Cieplak, P.; Bayly, C. I.; Gould, I. R.; Merz, K. M.; Ferguson, D. M.; Spellmeyer, D. C.; Fox, T.; Caldwell, J. W.; Kollman, P. A. A second generation force field for the simulation of proteins, nucleic acids, and organic molecules *J. Am. Chem. Soc*. **1995**, *117*, 5719−5197.
(58) Bayly, C. I.; Cieplak, P.; Cornell, W. D.; Kollman, P. A. A well-behaved electrostatic potential based method using charge restraints for deriving atomic charges. *J. Phys. Chem*. **1993**, *97*, 10269−10280.
(59) Case, D. A.; Darden, T. A.; Cheatham, T. E.; Pearlman, D. A.; Simmerling, C. L.; Wang, J.; Duke, R. E.; Luo, R.; Merz, K. M.; Pearlman, D. A.; Crowley, M.; Brozell, S.; Tsui, V.; Gohlke, H.; Mongan, J.; Hornak, V.; Cui, G.; Beroza, P.; Schafmeister, P.; Caldwell, J. W.; Ross, W. S.; Kollman, P. A. *AMBER*, version 8; University of California: San Francisco, CA, 2004.

JM0503289